Article

The Role of Sulfuric Acid, Abiotic–Organic Acids, and Biotic Acids on Serpentinite Dissolution and Trace Metal Release

Agnes R. Taylor [1], Amanda Albright Olsen [1],*, Elisabeth M. Hausrath [2], Brian J. Olsen [3] and Dawn Cardace [4]

1   School of Earth and Climate Science, University of Maine, Orono, ME 04469, USA; taylor.agnes.r@gmail.com
2   Department of Geoscience, University of Nevada, Las Vegas, NV 89154, USA; elisabeth.hausrath@unlv.edu
3   School of Biology and Ecology, University of Maine, Orono, ME 04469, USA; brian.olsen@maine.edu
4   Department of Geosciences, University of Rhode Island, Kingston, RI 02881, USA; cardace@uri.edu
*   Correspondence: amanda.a.olsen@maine.edu; Tel.: +1-207-581-2194

Abstract: Organic acids produced by biota have been shown to accelerate the dissolution of minerals, possibly creating biosignatures in either reacting solutions or the solid materials. We tested aqueous alteration of serpentinite in three groups of solutions: inorganic acids, organic acids created through abiotic processes (termed "abiotic–organics"), and organic acids created through biotic processes (termed "biotic acids") over a range of temperatures relevant to conditions on Mars and Europa. A total of 48 batch reactor experiments were carried out at 0 °C, 22 °C, and 62 °C in 16 different acids at pH 2.6 over 28 days. Additional experiments were conducted in sulfuric acid solutions to assess aqueous alteration in sulfate-rich environments. These results show that biotic acids accelerate serpentinite dissolution compared to the control inorganic acid, whereas abiotic–organic acids have little or no effect. Sulfuric acid enhances serpentinite dissolution over nitric acid. Secondary precipitates found in the presence of biotic acids were consistently enhanced in Mn, Ti, and W. We propose that these preferentially released elements and secondary minerals may be potential biosignatures. We also show that the release of the rock-forming elements Mg and Si is correlated with stability constants for the metal–acid aqueous complex, providing a possible mechanistic interpretation of the observed results.

Keywords: serpentinite; weathering; biosignatures; organic acids; aqueous alteration

1. Introduction

Serpentine, a phyllosilicate mineral that is commonly formed from aqueous alteration of Fe- and Mg-rich ultramafic parent materials [1], has been detected in multiple locations on Mars [2–8] and in meteorites [9,10], and is hypothesized to exist at interfaces between silicate mantles and liquid water oceans on Europa [11,12], Enceladus [13,14], and other ocean worlds [15]. Serpentine minerals are of particular interest in planetary exploration because they are documented habitable, extreme environments for microorganisms on Earth [16–24] and therefore are likely to represent bioenergetically rich niches in other planetary systems. Serpentinites are rocks dominated by serpentine minerals with the chemistry $Mg_3Si_2O_5(OH)_4$ with varying amounts of Fe, Ni, Al, Zn, and Mn substitutions. They often occur with smectite and chlorite group clay minerals, magnetite, brucite, carbonates, as well as possible primary unaltered olivine and pyroxene. In addition to having a low Ca to Mg ratio, serpentinites are rich in trace elements including Mn, Cr, Ni, and Co [25]. Serpentinites in planetary systems present unique metabolic opportunities over a wide range of temperatures. When serpentinites interact with aqueous solutions at lower temperatures, additional changes in the mineralogy and trace element mobility occur via low-temperature aqueous alteration [26,27]; these changes are influenced by factors including pH, duration of contact with water, and the composition of the surrounding water, including key organic ligands. The results of these interactions are preserved in the through-going waters and

newly formed secondary minerals. Although geologically old percolating fluids are largely lost to observation, durable mineral products and geochemical veneers persist and can be often key reservoirs of intact biosignatures in planetary settings.

On Earth, studies have shown that organic acids produced by microorganisms and plants enhance mineral dissolution rates in weathering environments [28–39]. In addition to accelerated dissolution, some trace elements may be preferentially released in the presence of organic acids during water–rock interaction [36,40–42], which may result in a preserved record of mineral–microbe interactions. These organic ligand-mineral reactions lead to changes in both the solution chemistry and the secondary mineralogy. Several mechanisms by which organic acids promote mineral dissolution have been proposed. Hausrath and collaborators [36] showed that release rates for primary elements in basalts and granites in the presence of an organic ligand correlate with measured stability constants for the organic ligand–element aqueous complex. This suggests that the enhancement in elemental release is due to how strongly the organic ligand can bond to and remove elements from the mineral structure. Similarly, Olsen and Rimstidt [35] suggested that oxalic acid increases forsterite dissolution rates compared to forsterite dissolution rates in inorganic solutions by more effectively complexing Mg^{2+} from the mineral structure [43,44]. Conversely, other studies have suggested that organic acids do not form inner sphere complexes with silica in tectosilicates and clays, suggesting that increased mineral dissolution rates in the presence of organic acids are caused by an indirect process such as increased ionic strength [45] or complexation of aqueous Al by organic ligands, thereby increasing solubility [46].

Although most organic molecules on Earth are produced by biota, organic molecules that are not produced through biotic processes are present in the solar system. Organic molecules have been found in comets and meteorites, particularly carbonaceous chondrites which on average contain 2 wt% organic carbon [47]. A large group of organic compounds including carboxylic acids, amino acids, and aliphatic and aromatic hydrocarbons have been detected in the CM Murchison meteorite [48]. A group of CR meteorites from Antarctica also contain a diverse and different suite of organic molecules, including larger concentrations of many water-soluble organics including ammonia [49]. The 1976 Viking expedition found no evidence of organics on Mars even though bombardment by meteorites should bring large concentrations of organic molecules to the Martian surface [50]. However, several instruments including Mars Express [51], Curiosity [52,53], and ground-based telescopes [54] have now detected low concentrations of methane (less than 30 ppbv) in the Martian atmosphere. The Curiosity Rover's Sample Analysis at Mars instrument has detected chlorinated hydrocarbons in the Sheepbed Mudstone [55]; thiophenic, aromatic, and aliphatic compounds the Mojave and Confidence Hill sites in the Murray Mudstone [56]; and benzoic acid, ammonia, phosphoric acid, and phenol at Bagnold Dunes [57]. Additionally, the Perseverance rover's SHERLOC instrument detected perchlorate and aromatic hydrocarbons using fluorescence and Raman spectroscopy in igneous ultramafic and basaltic rocks at Jezero Crater [58,59]. Organic material that is likely associated with carbonation and serpentinization has been detected in several Martian meteorites [60,61]. These findings suggest that organic molecules that are not created through biological processes are ubiquitous in the solar system. Based on these observations, it is not possible to assume that life was present in a planetary environment simply due to the detection of organic molecules. Therefore, we need the ability to distinguish between signatures of aqueous alteration that took place in the presence of biota from those formed through interaction with organic acids that are not associated with life.

In this study, we examine aqueous alteration and dissolution of serpentinite in the presence of a large group of organic acids that are commonly found in the solar system as a result of abiotic processes, biotic processes, or both with the goal of identifying differences in potential signatures created by each organic molecule. We hypothesize that aqueous geochemical reactions between water, serpentinite, and organic molecules generally formed through biotic processes (referred to as "biotic acids" in this study) produce chemical signatures distinct from reactions between water, serpentinite, and

organic molecules produced through abiotic processes (termed "abiotic–organic acids") and from those chemical signatures produced by a reference inorganic acid (e.g., nitric acid). In addition, we assess whether serpentinite alteration in sulfuric acid, which has been suggested to impact mineral dissolution [62] and is known to be abundant in many planetary systems including Mars [63] and Europa [64], proceeds differently than with nitric acid or organic acids of either class. We address these questions by completing a series of batch reactor experiments under targeted temperatures and conditions relevant to planetary surfaces and mantle–water interfaces. These experimental results specifically target three research questions: *(1) How does the dissolution of serpentinite vary in systems reacted with nitric acid, sulfuric acid, abiotic–organic acids, and biotic acids?; (2) do biotic acids facilitate the preferential release of certain cations from the rock structure over abiotic–organic or inorganic acids that may be used as biosignatures?; and (3) would these biosignatures be different in a high-sulfur environment?*

2. Materials and Methods

2.1. Materials

Serpentinized peridotite was collected from the Pine Hill Quarry on Little Deer Isle in the Penobscot Bay on the central Maine coast. The rock was characterized using X-ray diffraction (XRD), electron probe microanalysis (EPMA), and scanning electron microscopy (SEM) in previous work, and detailed discussion of the mineralogy and chemistry are included in Olsen and others [26] and Bodkin [65]. The rock is dominated by Mg-rich serpentine phase minerals (77%) and Ca- and Mg-rich augite (20%) with accessory magnetite (2%), chromite (0.5%), and trace amounts of ilmenite, apatite, millerite, titanite, and phlogopite [26]. The fresh rock was crushed and dry-sieved to 150–250 μm then cleaned by sonication in ethanol and dried in an oven at 40 °C for 24 h. A BET surface area of 0.9604 m^2/g was determined using the single-point N_2 method on a Micrometrics ASAP 2020 Surface Area Analyzer at the Laboratory for Surface Science and Technology at the University of Maine.

Sixteen acids were chosen as experimental solutions representing three distinct categories: (1) inorganic acids, defined as acids that are generally formed through inorganic processes and containing no carbon; (2) abiotic–organic acids, defined as acids containing covalently bonded carbon atoms that are known to form through non-biologic processes in planetary settings; and (3) biotic acids, defined as acids containing covalently bonded carbon atoms that are known to commonly form through biological processes on Earth (Table 1). Several acids, including acetic acid, glutamic acid, and formic acid, can be produced by both abiotic and biotic pathways [66–69]. For data analysis purposes, these were considered biotic acids due to their abundance in biotic systems. All initial solutions contained 0.01 M of one acid ligand (Table 1) and 0.05 wt% lithium azide to prevent microbial growth. Solutions were adjusted to an initial pH of 2.6 using either concentrated HCl or NH_4OH. No pH buffers were used due to previous evidence that they can affect dissolution rates and complexation within the experiments.

2.2. Experimental Design

A total of 48 experiments were conducted using each organic acid (Table 1) at pH 2.6 and three temperatures (0 °C, 22 °C, and 62 °C) to cover a wide range of alteration conditions. Experiments were run in FisherBrand® 250 mL polycarbonate flasks with caps containing 2 g of serpentinite and 200 mL of solution for 28 days. Experiments run at 22 °C and 62 °C were placed in a temperature-controlled Precision® Reciprocal Shaking Bath for the entirety of the experimental run to ensure temperature remained constant while consistently agitating the solution. Because of temperature limitations of the shaker bath, the 0 °C batch reactors were kept in coolers packed full of ice. Temperatures were monitored daily to ensure that temperatures stayed at 0 °C; solutions were also lightly shaken daily to ensure mixing. Any melt water in the cooler was drained daily and ice was refreshed every other day.

Table 1. Acid treatment used in batch reactor experiments accompanied by their chemical formula and the reasoning behind their selection.

Acid Treatment	Chemical Formula	Reason for Selection
Abiotic		
Nitric	HNO_3	inorganic control
Sulfuric	H_2SO_4	important in planetary systems
Abiotic–Organic		
Acetic *	$C_2H_4O_2$	found in carbonaceous chondrites
Glutamic *	$C_5H_9NO_4$	found in carbonaceous chondrites
Methanesulfonic	CH_4O_3S	found in carbonaceous chondrites
Nonanoic	$CH_3(CH_2)_7COOH$	found in carbonaceous chondrites
Valeric	$C_5H_{10}O_2$	found in carbonaceous chondrites
α-aminoisobutyric	$C_4H_9NO_2$	found in carbonaceous chondrites
Biotic		
Acetic *	$C_2H_4O_2$	produced by bacteria on Earth
Citric	$C_6H_8O_7$	produced by bacteria on Earth
Glutamic *	$C_5H_9NO_4$	produced by bacteria on Earth
Formic	CH_2O_2	produced by bacteria on Earth
Fumaric	$C_4H_4O_4$	produced by bacteria on Earth
Gluconic	$C_6H_{12}O_7$	produced by bacteria on Earth
Glycolic	$C_2H_4O_3$	produced by bacteria on Earth
Lactic	$C_3H_6O_3$	produced by bacteria on Earth
Malic	$C_4H_6O_5$	produced by bacteria on Earth
Oxalic	$C_2H_2O_4$	produced by bacteria on Earth

* Acetic and glutamic acid are listed under abiotic–organic and biotic subheadings due to their ability to be produced by both pathways. For the purpose of statistical analyses, both were considered biotic acids.

Approximately 5–6 mL of solution was sampled at 30 min, 3 h, 8 h, and 1, 2, 3, 5, 7, 10, 14, 21, and 28 days after the start of the experiment. Each sample was extracted with a sterilized syringe, pushed through a 0.22 μm filter, and stored in a sterilized polycarbonate sample bottle at 5 °C until analysis. Solutions were weighed and pH was measured using a Mettler Toledo SevenEasy® bench top meter.

2.3. Solution Chemistry

Solution chemistry was measured using a Thermo® ELEMENT2 high-resolution inductively coupled plasma-mass spectrometer (ICP-MS) (Waltham, MA, USA) at the Climate Change Institute at the University of Maine. Each sample solution was diluted 1:41.66, acidified to 1% HNO_3, and spiked with 2 ppb In. Each sample was run twice, once undiluted and then again after dilution. Concentrations of Al, Ba, Ca, Ce, Cd, Co, Cr, Cs, Cu, Fe, K, La, Mg, Mn, Mo, Na, Ni, P, Pb, Pr, Rb, S, Sc, Si, Sr, Th, Ti, U, V, W, Y, Zn, Zr were collected for each sample. Solution concentrations were corrected for the evolving solid to solution ratio using the method described in Olsen and Rimstidt [35]. Because the addition of lithium azide added measurable concentrations of many analytes to the solution, blanks were analyzed using ICP-MS and the measured concentrations were subtracted from experimental data.

2.4. Secondary Mineral Characterization

After completion of the experiments, solutions were decanted and reacted serpentinite was collected, dried in an oven at 40 °C, and stored at room temperature until analysis. The morphology and chemistry of the reacted grains and secondary precipitates were analyzed using a Tescan Vega XMU® scanning electron microscope with a EDAX Apollo® energy-dispersive X-ray detector (Warrendale, PA, USA) at the University of Maine. When substantial secondary precipitates were observed, the reacted grains were analyzed using

an Olympus TERRA® portable X-ray diffractometer (XRD) (Waltham, MA, USA) at the University of Rhode Island.

Reacted solutions were decanted and evaporated to dryness at 40 °C. The remaining fine-grained evaporites were analyzed by both XRD and qualitative X-ray fluorescence (XRF) using the TERRA XRD at the University of Rhode Island. The XRF feature operates at an energy resolution of 250 eV at 5.9 keV with an energy range from 3–25 keV and can detect elements from calcium to uranium.

2.5. Statistical Methods

We modeled concentration as a function of time, temperature, and acid type for each experiment using two separate, multiple linear regression models using function *lm* in the R Computing Environment [70]. We first log-transformed elemental concentration and time to meet the assumption of linearity for these models. The parameter estimates (β) of the regressions therefore simultaneously test (A) the linear relationship between time and elemental concentration, (B) the linear relationship between temperature and elemental concentration, and (C) the expected change in elemental concentration between acid type (defined in two ways as described below) and a reference type for a given time and temperature. We considered parameter estimates with $p < 0.05$ as statistically significant (different from no relationship) a priori.

Two statistical models were developed to address the three different research questions. Model 1 evaluated research question 1 (*How does the dissolution of serpentinite vary in systems reacted with nitric acid, sulfuric acid, abiotic–organic acids, and biotic acids?*) by testing for differences in log-elemental Mg or Si concentration among four acid groups: abiotic–organic acids (N = 6), biotic acids (N = 10), sulfuric acid (N = 1), and the control inorganic acid (nitric acid; N = 1). This model explicitly tests for differences between the average elemental release by these four groups. We selected Mg and Si because they are the two major rock-forming elements in both serpentine and pyroxene and are therefore the most appropriate elements for approximating bulk rock dissolution in serpentinite.

Model 2 similarly evaluated research question 2 (*Do biotic acids facilitate the preferential release of certain cations from the rock structure over abiotic–organic or inorganic acids that may be used as biosignatures?*) and research question 3 (*Would these biosignatures be different in a high sulfur environment?*) by evaluating the differential elemental release for 33 elements in the presence of the 16 acids used in the experiments. This model was run using elemental concentration data for each experiment for each of the following elements: Al, Ba, Ca, Ce, Cd, Co, Cr, Cs, Cu, Fe, K, La, Mg, Mn, Mo, Na, Ni, P, Pb, Pr, Rb, S, Sc, Si, Sr, Th, Ti, U, V, W, Y, Zn, and Zr. We used both nitric acid (Research Question 2) and sulfuric acid (Research Question 3) as inorganic acids to generate a list of elements preferentially released in the presence of an either abiotic–organic or biotic acids relative to these base line inorganic acids (controlling for time and temperature). Elements that are preferentially released in the presence of biotic acids but not abiotic–organic acids were then compared for potential use as biosignatures. We chose sulfuric acid as an experimental variable to reflect that many planetary systems are enriched in sulfur. Our model thus allows us to describe both a chemical signature for a general nitric acid environment and general sulfuric acid environment.

3. Results

3.1. Solution pH As a Function of Time

From an initial pH of 2.6 for each experiment, fluid chemistry evolved, and pH rose in every experiment (Supplementary Table S1). For the 0 °C experiments, the pH rose to a maximum of 6.40; for the 22 °C and 62 °C experiments, pH maxima occurred at 5.38 and 7.02, respectively. In all experiments, the pH rose quickly at first, then leveled off after two to three days.

3.2. Statistical Results

3.2.1. Statistical Results for Research Question 1 (Model 1): How Does the Dissolution of Serpentinite Vary in Systems Reacted with Nitric Acid, Sulfuric Acid, Abiotic–Organic Acids, and Biotic Acids?

Model 1 evaluated Mg or Si release against time in three acid categories (abiotic–organic, biotic, and sulfuric) compared to the control acid category (nitric acid). Residuals for Model 1 for both Mg and Si met the assumptions of linear models. Model fit was appropriate for both the Mg (adjusted $R^2 = 0.79$) and Si (adjusted $R^2 = 0.61$) models (Table 2). Model 1 shows that although Mg release in the presence of abiotic–organic acids is slightly higher than in the presence of nitric acid, it is not statistically different ($\beta \pm$ standard error $= 0.04 \pm 0.043$, $p = 0.300$; Figure 1). However, Mg release in the presence of biotic acids ($\beta = 0.25 \pm 0.041$, $p < 0.0001$) and sulfuric acid ($\beta = 0.23 \pm 0.055$, $p < 0.0001$) is significantly higher than in nitric acid (Figure 1).

Table 2. Multiple linear regression results for research question 1, used to evaluate Mg and Si release under four different acid conditions.

Acid Category	Parameter Estimate	Standard Error	*p*-Value
Magnesium			
Control–Nitric	−5.17	0.066	-
Sulfuric	0.23	0.055	<0.001
Abiotic–Organic	0.04	0.043	0.30
Biotic	0.25	0.041	<0.001
Silicon			
Control–Nitric	−5.08	0.079	-
Sulfuric	0.35	0.066	<0.001
Abiotic–Organic	0.14	0.051	0.00615
Biotic	0.25	0.049	<0.001
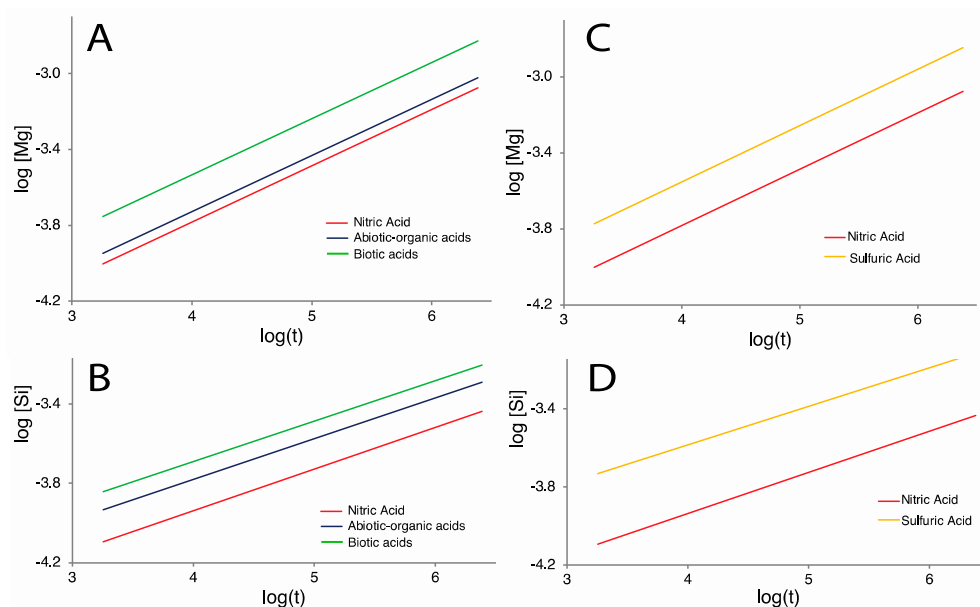
Figure 1. Regression results from Model 1 illustrate the increased Mg (**A**) and Si (**B**) release in the presence of biotic acids compared to abiotic-organic and inorganic acids as well as increased Mg (**C**) and Si (**D**) release in the presence of sulfuric acid compared to nitric acid.

Silicon release was significantly greater for all acid categories relative to nitric acid. Abiotic–organic acids released more silicon than nitric acid ($\beta = 0.14 \pm 0.051$, $p = 0.006$), followed by biotic acids ($\beta = 0.25 \pm 0.049$, $p < 0.0001$), and finally sulfuric acid sulfuric

acid ($\beta = 0.35 \pm 0.066$, $p < 0.0001$), which released the most silicon (Figure 1). All three test categories are significantly different from each other based on standard errors (Table 2).

3.2.2. Statistical Results for Model 2

Model 2 assesses preferential release of individual elements relative to an inorganic acid for each individual abiotic–organic and biotic acid. Model 2 was run separately using nitric and sulfuric acid as the comparison inorganic acid (nitric acid for research question 2; sulfuric acid for research question 3). This allows us to compare potential biosignatures for sulfur-rich and sulfur-poor environments, extending the usefulness of this analysis to a wide group of planetary systems. A tabulation of the elements for which each organic acid showed preferential release relative to the control acid (i.e., significant, positive β-values) is presented in Table 3 for nitic acid and Table 4 for sulfuric acid. The residuals for Model 2 met the assumptions of linear models with appropriate model fit, although a few elements (K, Na, Pb, P, and Zn) were poorly explained by the model (mean $R^2 \pm$ standard error = 0.22 ± 0.03). Resulting *p*-values for each acid–cation pair, which describe the y-intercepts of each acid compared to the inorganic acid, are presented in Supplementary Table S2 for Research Question 2 and Supplementary Table S3 for Research Question 3. R^2 values are presented in Supplementary Table S4.

Table 3. A tabulation of all statistically significant (*p*-value < 0.05) elements with positive β-values for each acid compared to nitric acid for research question 2.

Acid	Enhanced Elements
Inorganic	
Sulfuric	Al, Ca, Cd, Co, Cr, K, Mg, Mo, P, Pb, Rb, S, Sc, Si, Th, Ti, U, V, W, Y, Zr
Abiotic–organic	
2-Aminoisobutyric	Al, Ce, Co, Cr, Cu, Fe, Mn, Mo, Ni, Pb, Pr, Sc, Ti, U, V, Y
Methanesulfonic	Al, Pb, S, Si, Th, Ti, U, V, Zr
Nonanoic	Ca, Cd, Ce, Cr, K, Mo, Na, P, Pb, Pr, S, Th, U, W, Y, Zr
Valeric	Cd, Co, Cr, Cu, Fe, Mn, Na, Pb, Sc, U, Zn, Zr
Biotic	
Acetic	Cd, Ce, Co, Cr, Cu, Fe, Mn, Mg, Mo, Na, Pb, Sc, Si, Th, U, V
Citric	Al, Ca, Cd, Ce, Co, Cr, Cu, Fe, La, Mg, Mn, Mo, Ni, P, Pb, Pr, S, Sc, Si, Th, Ti, U, V, W, Y, Zr
Formic	Al, Cd, Ce, Co, Cr, Cu, Fe, La, Mg, Mn, Mo, Ni, Pb, Pr, Sc, Si, Th, Ti, U, V, Y, Zn
Fumaric	Al, Cd, Ce, Co, Cr, Cu, Fe, La, Mg, Mn, Mo, Ni, Pb, Pr, S, Sc, Si, Th, Ti, U, V, W, Y, Zr
Gluconic	Al, Ce, Cr, Cu, Mo, P, Pb, Pr, Sc, Th, Ti, U, V, Y, Zr
Glutamic	Al, Ce, Co, Cr, Cu, La, Mo, Pb, Pr, S, Sc, Si, Th, Ti, U, V, W, Zr
Glycolic	Al, Cd, Ce, Co, Cr, Cu, Fe, La, Mg, Mn, Mo, Ni, Pb, Pr, S, Sc, Si, Th, Ti, U, V, W, Y, Zn, Zr
Lactic	Al, Ce, Co, Cr, Cu, Fe, La, Mg, Mn, Mo, Na, Pb, Pr, Sc, Si, Th, Ti, U, V, W, Y, Zr
Malic	Al, Ca, Cd, Ce, Co, Cr, Cu, Fe, La, Mg, Mn, Mo, Ni, P, Pb, Pr, Sc, Si, Th, Ti, U, V, W, Y, Zr
Oxalic	Al, Ca, Ce, Co, Cr, Cs, Fe, La, Mg, Mo, Ni, P, Pb, Pr, S, Sc, Si, Th, Ti, U, V, W, Y, Zr

Model 2 Results for Research Question 2: Do Biotic Acids Facilitate the Preferential Release of Certain Cations from the Rock Structure over Abiotic–Organic or Inorganic Acids That May Be Used as Biosignatures?

For Research Question 2, at least one acid from both the abiotic–organic and biotic categories produced statistically significant higher release rates than nitric acid for every element that was analyzed (Table 3). Likewise, all acids in both categories produced release rates that were statistically higher than nitric acid for at least one element. In the case of U and Pb, all acids resulted in greater elemental release than nitric acid. No acid consistently increased the release of all elements relative to nitric acid.

Although the abiotic–organic acids had a relatively high number of preferentially released elements, only two (U and Pb) were preferentially released by all the abiotic–organic acids. However, both elements were preferentially released by all the biotic acids as well and therefore would not be useful for identifying a chemical signature produced by

abiotic–organic acids. One element (K) was preferentially released only by abiotic–organic acids. Model performance for K, however, was poor (adjusted $R^2 = 0.30$).

Table 4. All statistically significant (*p*-value < 0.05) elements with positive β-values for each acid compared to sulfuric acid for Research Question 3.

Acid	Enhanced Elements
Inorganic	
Nitric	Ba, Sr
Abiotic–organic	
2-Aminoisobutyric	Ba, Cs, Cu, Sr, U
Methanesulfonic	Al, Ba
Nonanoic	Ba, W, Zn
Valeric	Ba, Cu, Sr
Biotic	
Acetic	Mn
Citric	Al, Ba, Ca, Ce, Co, Cr, Cu, Fe, La, Mg, Mn, Mo, Ni, P, Pb, Pr, Sc, Th, Ti, V, W, Y, Zr
Formic	Al, Ba, Ce, Co, Cr, Cu, La, Pb, U, V, Zn
Fumaric	Al, Ba, Co, Cr, Cu, Fe, Mn, Pb, Sc, Ti, U, V, W, Zr
Gluconic	Al, Ba, Cr, Cu, Mo, Pb, Sc, Th, Ti, V, W, Zr
Glutamic	Al, Ba, Ce, Cr, Cu, La, Pb, Pr, Ti, U, V
Glycolic	Ba, Cr, Cu, Mo, Pb, Sc, Th, Ti, V, W, Zr
Lactic	Al, Ba, Ce, Cr, Cu, Mo, Pb, Pr, Sc, Ti, V, W, Zr
Malic	Al, Ba, Ce, Co, Cr, Cu, Fe, La, Mg, Mo, Pb, Pr, Sc, Th, Ti, V, W, Y, Zr
Oxalic	Al, Ba, Ce, Co, Cr, Cs, La, Mg, P, Pb, Pr, Sc, Sr, Th, Ti, V, W, Y, Zr

Biotic acids showed preferential release relative to nitric acid for a range of elements (Table 3). Specifically, Ce, Cr, Mo, Pb, Sc, Th, U, and V were preferentially released by all the biotic acids (although each one was also preferentially released by at least one abiotic–organic acid). Cs, La, and Mg were only preferentially released by biotic acids, although these were not preferentially released by all biotic acids.

Statistical Results for Research Question 3 (Model 2B): Would these Biosignatures Be Different in a High-Sulfur Environment?

Research Question 3 evaluates preferential release from organic acids compared to sulfuric acid to address the possibility that high sulfur concentrations may affect biosignatures. Fewer elements showed preferential release in the presence of abiotic–organic or biotic acids compared to sulfuric acid than in the presence of nitric acid, although all acids in both organic categories showed preferential release of at least one element over sulfuric acid (Table 4). Several elements (Cd, K, Na, Rb, and Si) did not show preferential release in any acid over sulfuric acid. Few elements (Al, Ba, Cs, Cu, Sr, U, W, and Zn) showed preferential release in any of the abiotic–organic acids over sulfuric acid. Barium showed preferential release over sulfuric acids in all four abiotic–organic acids. No acid consistently increased the release of all elements relative to sulfuric acid.

The chemical signature of biotic acids relative to sulfuric acid differed from that of nitric acid. Multiple elements (Al, Ba, Ca, Ce, Co, Cr, Cs, Cu, Fe, La, Mg, Mn, Mo, Ni, P, Pb, Pr, Sc, Sr, Th, Ti, U, V, W, Y, Zn, and Zr; Table 4) show preferential release in the presence of at least one biotic acid compared to release in sulfuric acid. However, several of these elements (Al, Ba, Cs, Cu, Sr, U, W, and Zn) also show preferential release in the presence of at least one abiotic–organic acid. Twenty elements (Ba, Ca, Ce, Co, Cr, Fe, La, Mg, Mn, Mo, Ni, P, Pb, Pr, Sc, Th, Ti, V, Y, and Zr) are therefore released at higher concentrations only in the presence of biotic acids relative to sulfuric acid.

### 3.3. Characterization of Secondary Precipitates

Although solution chemistry can shed light on potential secondary mineral formation, solution chemical signatures might be most relevant for ocean worlds such as Europa. In order to assess secondary mineral formation that might be more relevant to secondary mineral formation during weathering in systems such as Mars, we also include a characterization of the secondary precipitates observed in this study, although the detection limits are not as sensitive as solution detection limits. However, the capabilities of the TERRA XRD system are comparable to what has historically been available on flight instruments, making this level of analysis appropriate and useful for this study. SEM images of unreacted serpentinite grains reveal surface morphologies that are variable and rough in nature (Supplementary Figure S1). Unreacted serpentine and augite grains frequently had inclusions rich in Cr, Ni, and Ti, which varied in morphology from needle-like polygons to curved features. Reacted serpentinite grains looked morphologically like the unreacted grains with a similar surface roughness. No unique morphological changes were detected between the inorganic, abiotic–organic, or biotic acid treatments.

Growth of secondary precipitates on or between reacted grains was identified in 27 of 48 experiments. Precipitates were found as interstitial growths, coatings on grain surfaces, fibrous meshes, and globular mats (Figure 2). The relative concentration of precipitates was higher in the abiotic–organic and inorganic acid treatments in comparison to the biotic acid treatments. Additionally, the abundance of secondary precipitates qualitatively increases as temperature increases. We attempted to identify precipitate mineralogy using XRD but were unable to due to low total precipitation mass. Two chemically distinct secondary precipitates were identified using SEM-EDS. The most common precipitate was rich in Fe and O and appeared in experiments from all acid categories. This Fe-rich compound grew interstitially and as coatings on rock grains (Figure 2). The morphology of these oxides varied as interstitial, platy rock coatings, fibrous meshes, and globular mats. A second precipitate that is rich in Mg and O was precipitated in the presence of oxalic acid at 62 °C (Figure 3). This Mg-rich precipitate occurs as a cubic morphology and was relatively abundant, growing both interstitially and atop grains, although the latter was more common. This precipitate was not found in large enough quantities to be identified by XRD but is likely a Mg oxide or Mg oxalate phase.

Twenty-two experiments yielded enough suspended precipitate volume for characterization using qualitative XRF (Table 5). Solutions at the end of experimentation varied in color and opacity (Supplementary Figure S2). The isolated suspended particles varied in texture from tacky to granular, and varied in color from brown, orange, and green. All suspended precipitates contained Fe regardless of acid category and temperature (Table 5). Chromium was detected in all samples except for the glutamic acid experiment run at 22 °C. Calcium was detected in 11 of the experiments for which precipitates were collected. Cobalt was detected in two abiotic–organic experiments (methanesulfonic acid at 22 °C and nonanoic acid at 0 °C). Titanium was detected in the 0 °C malic acid and the high-temperature oxalic acid experiment. Manganese was detected in the 22 °C fumaric acid experiment as well as the 62 °C oxalic acid experiment. Tungsten was identified in precipitates from the 0 °C fumaric acid and glutamic acid experiments. Cl was found in almost all experiments and is attributed to the use of HCl acid to adjust the initial pH of the solutions. No Si was detected, suggesting that most of the secondary minerals are iron oxides. Substitution within the goethite structure is common, especially for trivalent metal ions [71]. It is possible that the signal for Cr and Mn was from these metals substituted into the goethite structure and that the identified Ca, Cr, Mn, Ti, and W were adsorbed onto the reactive mineral surface.
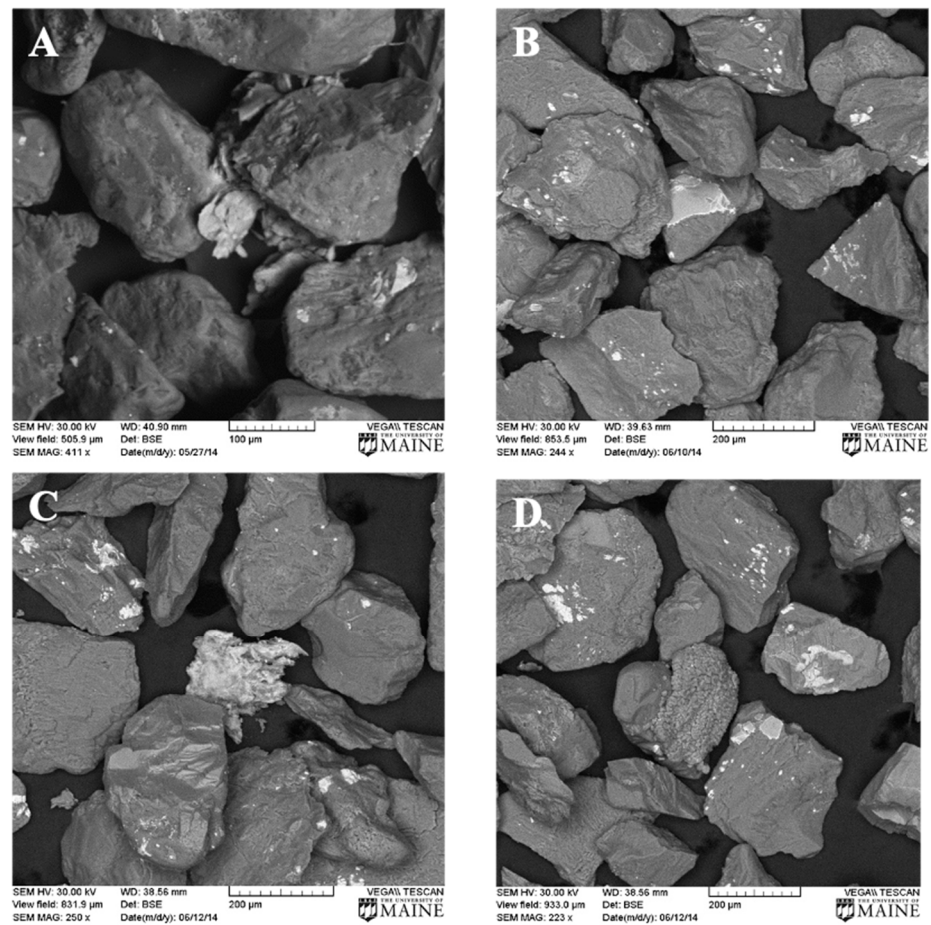
Figure 2. Photomicrograph of the four different growth behaviors of the secondary iron oxide including (**A**) interstitial growth; (**B**) coating a grain surface; (**C**) fibrous mesh textures; and (**D**) globular mats.
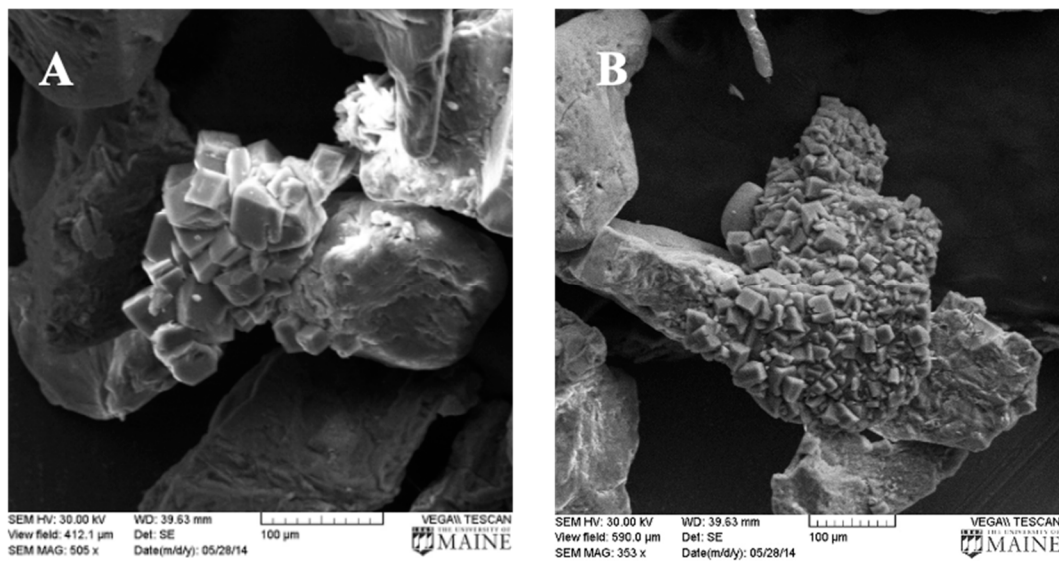
Figure 3. Photomicrograph of magnesium phase found as a secondary precipitate in the high-temperature oxalic acid experiment. (**A**) An example of interstitial growth behavior. (**B**) An example of the growth on top of grains.

Table 5. A tabulation of the experimental precipitates which were analyzed using qualitative XRF along with the elements detected.

Acid Treatment	Temperature (°C)	Detected Elements
Inorganic		
Nitric	62	Ca, Cl, Cr, Fe
Sulfuric	0	Ca, Cl, Cr, Fe
Abiotic–Organic		
Methanesulfonic	22	Co, Cr, Fe
Nonanoic	0	Co, Cr, Fe
Valeric	62	Ca, Cl, Cr, Fe
α-aminoisobutyric	0	Cl, Cr, Fe
α-aminoisobutyric	62	Cr, Fe
Biotic		
Acetic	0	Ca, Cl, Cr, Fe
Citric	0	Ca, Cl, Cr, Fe
Formic	0	Cl, Cr, Fe
Fumaric	0	Ca, Cl, Cr, Fe, W
Fumaric	22	Ca, Cl, Cr, Fe, Mn
Gluconic	0	Cl, Cr, Fe
Glutamic	0	Ca, Cl, Cr, Fe, W
Glutamic	22	Fe
Glycolic	0	Cl, Cr, Fe
Lactic	0	Ca, Cl, Cr, Fe
Malic	0	Ca, Cl, Cr, Fe, Ti
Oxalic	62	Ca, Cl, Cr, Fe, Mn, Ti

4. Discussion

4.1. Biotically Enhanced Serpentinite Dissolution

Results from Model 1, designed to test differences in serpentinite reactivity in inorganic, abiotic–organic, and biotic systems, show that across a wide range of temperatures, Mg and Si release from serpentinite in the presence of biotic acids is significantly enhanced compared with Mg and Si release in the presence of nitric acid (Figure 1A,B; Table 2). This is consistent with previous laboratory and terrestrial field studies that show that organic acids accelerate mineral weathering [28–39].

Assessing whether serpentinite dissolution is enhanced in the presence of abiotic–organic acids is more complicated. Mg release, as a proxy for whole-rock dissolution, in the presence of abiotic–organic acids does not significantly differ from Mg release in the presence of nitric acid (p-value = 0.29805; Table 2; Figure 1A), suggesting that unlike organic acids that are produced biotically, abiotic–organic acids do not accelerate mineral weathering. However, Si release in the presence of abiotic–organic acids, another proxy for whole-rock dissolution, is statistically different from Si release in the presence of nitric acid (p-value < 0.05; Table 2; Figure 1B), although the magnitude of the effect is substantially lower than the effect from biotic acids (parameter estimate = 0.14). The difference between the biotic regression line and the regression line of nitric acid is approximately two times larger than the difference between the abiotic–organic and nitric regression lines (Figure 1B). This suggests that while abiotic–organic acids may also slightly enhance mineral dissolution rates over nitric acid, the effect is minimal compared to the effect of biotically produced acids.

Therefore, although it is well established that organic acids accelerate mineral dissolution for a wide range of minerals, this study is the first to demonstrate that the organic acids that are produced by biota cause minerals to dissolve faster than organic acids that can be produced abiotically (Figure 1A,B). This study covers only one rock type (serpentinite) under a narrow range of environmental conditions (low pH; T = 0, 22, and 62 °C); however, a similar effect may occur with other minerals.

4.2. Sulfuric Acid Enhances Serpentinite Dissolution

Reaction in sulfuric acid environments enhances serpentinite dissolution relative to dissolution in nitric acid as much or more than reaction in the presence of abiotic–organic or biotic acids (Figure 1C,D). Previous experimental work has shown that the addition of sulfate to solutions does not accelerate the dissolution of Mg-rich olivines after controlling for the effect of pH [62]. However, this study shows that both Mg and Si release from serpentinite in sulfuric acid solutions are statistically greater than in nitric acid solutions (p-value < 0.05; Table 3, Figure 1D). The magnitude of the effect is greater for silica, which is consistent with the pattern observed in abiotic–organic and biotic acids. This suggests that overall serpentinite reactivity may be enhanced in sulfur-rich environments; however, further work is necessary to identify a mechanistic interpretation of this enhanced release.

4.3. Preferential Release of Trace Elements in Abiotic–Organic and Biotic Environments: Potential Biosignatures

In addition to testing whether biotic and abiotic–organic acids preferentially dissolve serpentinite, we also tested whether a large suite of major and trace elements are preferentially released during water–rock interaction in the presence of abiotic–organic and biotic acids relative to two inorganic acids, nitric acid and sulfuric acid, meant to simulate low- and high-sulfate environments. The results of our linear regressions show preferential release for a wide variety of elements in comparison to their release in the presence of two inorganic acids (Tables 3 and 4). By establishing which elements are preferentially released in the presence of biotic acids, we identify two possible chemical signatures that may be present in solutions that have experienced water–rock–biota interactions, as well as suggestions about the formation of possible secondary minerals that might be present under these conditions. However, we tested a large group of biotic and abiotic–organic acids, and not all acids from each group showed similar elemental release patterns, complicating identification of potentially useful chemical signatures.

In sulfate-free experiments, no single element was preferentially released by all biotic acids but not by the inorganic acid (Figure 4). Cesium, La, and Mg were preferentially released in the presence of at least one biotic acid but never in the presence of the abiotic–organic acids. Cesium was only preferentially released by oxalic acid. La was preferentially released by all biotic acids except for acetic and gluconic acid, whereas Mg was preferentially released by all biotic acids except for glutamic and gluconic. We also found that all biotic acids preferentially released Ce, Cr, Mo, Pb, Sc, Th, U, and V, although these were all preferentially released by at least one abiotic–organic acid. This suggests that Ce, Cs, Cr, La, Mg, Mo, Pb, Sc, Th, U, and V may be suitable chemical signatures indicative of an environment where biotically produced organic acids are present. The only elements that were preferentially released from the serpentinite structure by all abiotic–organic acids were U and Pb; however, U and Pb were also preferentially released in all the biotic experiments as well as the sulfuric acid experiments. Therefore, preferential release of U and Pb is likely from both abiotic and biotic pathways and is not a unique identifier of rock weathering by abiotic–organic acids. Consequently, these results suggest that there are no elements which are preferentially released from the serpentinite structure only in the presence of abiotic–organic acids.

In experiments containing sulfate, a large suite of elements including Ca, Ce, Co, Cr, Fe, La, Mg, Mn, Mo, Ni, P, Pb, Pr, Sc, Th, Ti, V, Y, and Zr were preferentially released in the presence of at least one biotic acid and never in the presence of the abiotic–organic acids or nitric acid (Figure 4). We also found that all biotic acids with the exception of acetic acid preferentially released Ba, Cr, Pb, and V. Acetic acid only preferentially released Mn compared to the release observed in the presence of sulfuric acid. However, acetic acid can be produced by both biotic and abiotic pathways. This suggests that Ba, Ca, Ce, Co, Cr, Fe, La, Mg, Mn, Mo, Ni, P, Pb, Pr, Sc, Th, Ti, V, Y, and Zr may be a suitable chemical signature indicative of a sulfur-rich environment where biotically produced organic acids are present. The only element found to be preferentially released by all the abiotic–organic

acids was Ba. However, Ba was also found to be preferentially released by all acids used in experimentation except for nitric and acetic acid. Therefore, the preferential release of Ba is likely to occur in the presence of organic acids produced by both biotic and abiotic pathways and is not a unique chemical signature for rock dissolution in the presence of abiotic–organic acids.

Figure 4. Potential chemical signatures of inorganic environments (blue) and abiotic–organic environments (purple) compared to potential biosignatures (green) observed in both solid precipitates and in solutions.

Although we see abundant differences in solution chemistry for experiments conducted in different acid categories, only secondary minerals remain for examination in many planetary environments of interest such as Mars. Some 27 of the 48 experiments yielded enough precipitates to characterize differences in secondary mineralization chemistry (Table 5; Figure 4). There were some trends cross all acids and temperatures; for instance, all precipitates contained Fe and none contained Si, and most contained Cr and Ca as well as Cl, which was present in initial solutions. Precipitates from inorganic experiments do not contain any elements not found in precipitates from organic experiments. However, only abiotic–organic experiments produced precipitates containing Co, and only biotic experiments produced precipitates containing Mn, Ti, and W. Although these elements were not found in each precipitate from these acid categories, this observation nonetheless provides a starting place for future investigation of solid biosignatures to distinguish between environments containing organic acids of abiotic or biotic origin.

4.4. Broader Implications for Mineral Stability in the Presence of Organic Acids

Previous work has suggested that the mechanism for enhanced mineral dissolution in the presence of organic acids may be related to the strength of the bond between the metal ion being liberated from the mineral structure and the organic ligand in solution over the less strong complexation of metal ions to H^+ in inorganic solutions [36,41,42,72,73]. Hausrath, Neaman and Brantley [36] applied this to potential biosignatures and showed that major and trace element release from basalt and granite is correlated with the metal–citrate stability constants, which is essentially the equilibrium constant for the formation of a complex in solution, and suggested that elements that are preferentially released can be used as biosignatures. To test whether elemental release patterns in serpentinite can be explained based on a stability constant with the goal of using this to help develop a predictive model for biosignatures, we tested whether elemental release is correlated with stability constants for organic acids complexing with six metals: Mg, Ca, K, Mn, Cu, and Ni. Although it would be hypothetically possible to carry out this analysis for all metal–organic ligand pairs measured in these experiments, stability constants are empirical and have not been measured for all metal–ligand pairs; therefore, we selected elements for which at least six metal–organic ligand stability constants were readily available in the

literature [74]. Because stability constants are highly sensitive to temperature and ionic strength, only experiments from this study that were conducted at 22 °C were included in this analysis, and stability constants measured between 20 and 25 °C were selected from the literature. Moreover, only experiments run at 25 °C were included in the analysis. Stability constants measured at ionic strengths between 0 and 0.1 were selected for analysis, since experimental solutions were relatively dilute. Release ratios $\left(R_{\frac{organic}{nitic}} \right)$ were calculated using the following expression

$$R_{\frac{organic}{nitic}} = \frac{M_{metal,org}}{M_{metal,nitric}} \tag{1}$$

where $M_{metal,org}$ is the total amount of an element of interest released in an organic acid solution over the 28 day experiment and $M_{metal,nit}$ is the total amount of an element of interest released in the organic–free nitric acid solution under the same conditions. Release ratios were then compared to empirical stability constants ($K_{Metal:ligand}$) using a simple linear regression. All experimental data, stability constants, and conditions used in this analysis are included in Supplementary Table S5, and parameter estimates and R^2 values for each regression are included in Supplementary Table S6. Release ratios for experiments conducted in sulfuric acid were consistently high and were removed from the analysis.

Of the six metals that we were able to analyze, the correlation between stability constant and ratio of release was strongest for Mg and Ca (Figure 5; Supplementary Table S6), two important elements in serpentine and augite, respectively, which make up the bulk of this serpentinite. In both cases, citric acid and oxalic acid had the highest stability constants and most metal released from the mineral structure. MgO makes up approximately 35% of the rock on average; therefore, any mechanism that preferentially releases Mg will speed up weathering of the whole rock. While CaO makes up only about 5% of the rock, it is primarily found in augite, which has been shown to weather more quickly than the more abundant serpentine minerals [26,27], meaning that preferential release of Ca may disproportionally result in disaggregation of the rock. We were not able to assess Si and Fe, the two other dominant elements in this rock. Si was not assessed due to lack of stability constants in the literature. Although stability constants for Fe are available, Fe occurs in both the Fe^{2+} and Fe^{3+} forms in serpentinites, making it impossible to compare to one stability constant.

Although a correlation was observed between stability constant and elemental release for the major rock-forming elements, no correlation was observed between stability constant and elemental release across a range of organic acids for the four trace elements that we were able to assess (Supplementary Figures S3–S6; Supplementary Table S6). Qualitatively, Cu shows slight enhancement in release in all organic acids compared to nitric acid regardless of the stability constant, which may suggest that redox conditions control the dissolution of Cu-containing sulfur minerals to a greater degree than ligand identity [41,42]. Neither Mn or Ni release show little to no enhancement due to organic acid compared to the nitric acid. Interestingly, K shows a decrease in release of one to two orders of magnitude in the presence of organic acids, but the K dataset is small, so it is difficult to draw any conclusions.

These results suggest that while organic acids do facilitate dissolution of serpentinite (Model 1) as well as greater release of many trace elements (Model 2), trace element release may not always be explained through empirical stability constants. It is possible that the process of trace element release will be driven more by the relationship between the stability constant and the dominant rock-forming elements, and that dissolution kinetics will also play a role in rocks with several minerals [36]; the oxidation state may also play a role for redox-sensitive elements [41,42]. Because this study addressed whole-rock dissolution for direct comparisons to field planetary studies, the geochemical data combine the dissolution processes of several minerals, which complicates mechanistic interpretations. Future work should focus on a model mineral system such as olivine or augite to more

effectively highlight differences between different acids, stability constants, and mineral dissolution rates.
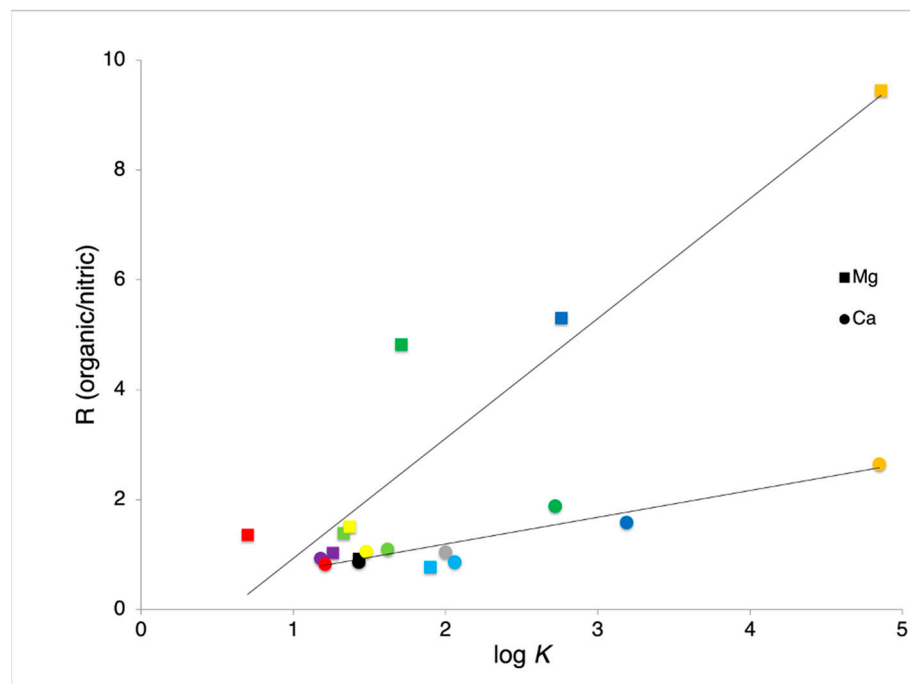
Figure 5. Release ratios for Mg and Ca in organic solutions and nitric acid versus the stability constant for the metal–ligand pair. Colors signify the acid of interest: red = gluconic acid; purple = acetic acid; black = formic acid; light green = glycolic acid; yellow = lactic acid; light blue = glutamic; gray = fumaric acid; dark green = malic acid; dark blue = oxalic acid; orange = citric acid.

5. Conclusions

Secondary minerals and solutions produced during aqueous alteration reactions provide unique records of serpentinite alteration by distinct aqueous solutions and bring new interpretive power to observations of extraterrestrial serpentinites. This work tests the hypothesis that major and trace element release during aqueous reactions between water, serpentinite, and biotic acids can be distinguished from elemental release during reactions between abiotic–organic acids, serpentinite, and water. We show that biotic acids release both Mg and Si faster than nitric acid alone, whereas abiotic–organic acids show only a small or inconclusive enhancement. Sulfuric acid enhances both Mg and Si release more than either of the organic acid categories, suggesting that dissolution reactions proceed more quickly within sulfur-rich systems such as Mars and Europa. We show a correlation between the release of major rock-forming elements Mg and Ca and the empirical stability constants for the metal–ligand complex in solution. However, no correlation was present for trace metal release.

Patterns in element release into solution and elemental retention in secondary minerals may be useful as potential biosignatures for the planetary science and astrobiology communities. When compared to elemental release in nitric acid solutions, we found that all biotic acids preferentially released Ce, Cr, Mo, Pb, Sc, Th, U, and V, into solution, although these were all also preferentially released by at least one abiotic–organic acid. When compared to elemental release in sulfuric acid, a large suite of elements including Ca, Ce, Co, Cr, Fe, La, Mg, Mn, Mo, Ni, P, Pb, Pr, Sc, Th, Ti, V, Y, and Zr were preferentially released in the presence of at least one biotic acid and never in the presence of the abiotic–organic acids, although preferential release was highly variable across the suite of biotic acids. Secondary precipitates included Fe, Ca, and Cr across all acid categories. Precipitates formed in inorganic experiments do not contain any elements not found in organic experiments. Some abiotic–organic experiments produced precipitates containing

Co, whereas some biotic experiments produced precipitates containing Mn, Ti, and W. These lines of evidence suggest that we have the potential to identify previously inhabited extraterrestrial environments through either solid or solution samples even if biota are no longer present.

Author Contributions: Conceptualization, A.A.O., A.R.T., E.M.H. and D.C.; methodology, A.A.O., A.R.T. and E.M.H.; software, A.R.T. and B.J.O.; validation, A.A.O., A.R.T. and B.J.O.; formal analysis, A.A.O., A.R.T. and B.J.O.; investigation, A.A.O., A.R.T., E.M.H. and D.C.; resources, A.A.O.; data curation, A.A.O. and A.R.T.; writing—original draft preparation, A.A.O., A.R.T. and B.J.O.; writing—review and editing, A.A.O., A.R.T., E.M.H., B.J.O. and D.C.; visualization, A.A.O., A.R.T., E.M.H., B.J.O. and D.C; supervision, A.A.O.; project administration, A.A.O.; funding acquisition, A.A.O. All authors have read and agreed to the published version of the manuscript.

Data Availability Statement: Taylor, Agnes; Olsen, Amanda; Hausrath, Elisabeth; Olsen, Brian; Cardace, Dawn (2024), "The role of sulfuric acid, abiotic–organic acids, and biotic acids on serpentinite dissolution and trace metal release", Mendeley Data, V2, doi: 10.17632/gkhjk3sz9x.2, accessed on 25 February 2024.

Conflicts of Interest: The authors declare no conflicts of interest. The funders had no role in the design of the study; in the collection, analyses, or interpretation of data; in the writing of the manuscript; or in the decision to publish the results.

References

1. Moody, J.B. An experimental study on the serpentinization of iron-bearing olivines. *Can. Mineral.* **1976**, *14*, 462–478.
2. Ehlmann, B.L.; Mustard, J.F.; Clark, R.N.; Swayze, G.A.; Murchie, S.L. Evidence for low-grade metamorphism, hydrothermal alteration, and diagenesis on Mars from phyllosilicate mineral assemblages. *Clays Clay Miner.* **2011**, *59*, 359–377. [CrossRef]
3. Ehlmann, B.L.; Mustard, J.F.; Murchie, S.L. Geologic setting of serpentine deposits on Mars. *Geophys. Res. Lett.* **2010**, *37*. [CrossRef]
4. Ehlmann, B.L.; Mustard, J.F.; Swayze, G.A.; Clark, R.N.; Bishop, J.L.; Poulet, F.; Des Marais, D.J.; Roach, L.H.; Milliken, R.E.; Wray, J.J.; et al. Identification of hydrated silicate minerals on Mars using MRO-CRISM: Geologic context near Nili Fossae and implications for aqueous alteration. *J. Geophys. Res. Planets* **2009**, *114*. [CrossRef]
5. Quantin, C.; Flahaut, J.; Clenet, H.; Allemand, P.; Thomas, P. Composition and structures of the subsurface in the vicinity of Valles Marineris as revealed by central uplifts of impact craters. *Icarus* **2012**, *221*, 436–452. [CrossRef]
6. Wang, A.; Crumpler, L.; Farrand, W.H.; Herkenhoff, K.E.; de Souza, P., Jr.; Kusack, A.G.; Hurowitz, J.A.; Tosca, N.J.; Korotev, R.L.; Jolliff, B.L.; et al. Evidence of phyllosilicates in Wooly Patch, an altered rock encountered at West Spur, Columbia Hills, by the Spirit rover in Gusev crater, Mars. *J. Geophys. Res. Planets* **2006**, *111*. [CrossRef]
7. Bristow, T.F.; Grotzinger, J.P.; Rampe, E.B.; Cuadros, J.; Chipera, S.J.; Downs, G.W.; Fedo, C.M.; Frydenvang, J.; McAdam, A.C.; Morris, R.V.; et al. Brine-driven destruction of clay minerals in Gale crater, Mars. *Science* **2021**, *373*, 198–204. [CrossRef] [PubMed]
8. Simon, J.I.; Hickman-Lewis, K.; Cohen, B.A.; Mayhew, L.E.; Shuster, D.L.; Debaille, V.; Hausrath, E.M.; Weiss, B.P.; Bosak, T.; Zorzano, M.-P.; et al. Samples Collected from the Floor of Jezero Crater with the Mars 2020 Perseverance Rover. *J. Geophys. Res. Planets* **2023**, *128*, e2022JE007474. [CrossRef]

9. Hicks, L.J.; Bridges, J.C.; Gurman, S.J. Ferric saponite and serpentine in the nakhlite martian meteorites. *Geochim. Cosmochim. Acta* **2014**, *136*, 194–210. [CrossRef]

10. Bass, M.N. Montmorillonite and serpentine in orgueil meteorite. *Geochim. Cosmochim. Acta* **1971**, *35*, 139–147. [CrossRef]

11. Vance, S.; Harnmeijer, J.; Kimura, J.; Hussmann, H.; Demartin, B.; Brown, J.M. Hydrothermal systems in small ocean planets. *Astrobiology* **2007**, *7*, 987–1005. [CrossRef]

12. Lowell, R.P.; Dubose, M. Hydrothermal systems on Europa. *Geophys. Res. Lett.* **2005**, *32*, 4–7. [CrossRef]

13. Czechowski, L. Some remarks on the early evolution of Enceladus. *Planet. Space Sci.* **2014**, *104*, 185–199. [CrossRef]

14. Malamud, U.; Prialnik, D. Modeling serpentinization: Applied to the early evolution of Enceladus and Mimas. *Icarus* **2013**, *225*, 763–774. [CrossRef]

15. Vance, S.D.; Daswani, M.M. Serpentinite and the search for life beyond Earth. *Philos. Trans. R. Soc. A-Math. Phys. Eng. Sci.* **2020**, *378*, 20180421. [CrossRef] [PubMed]

16. Cardace, D.; Hoehler, T.M. Serpentinizing Fluids Craft Microbial Habitat. *Northeast. Nat.* **2009**, *16*, 272–284. [CrossRef]

17. McCollom, T.M.; Seewald, J.S. Serpentinites, Hydrogen, and Life. *Elements* **2013**, *9*, 129–134. [CrossRef]

18. Schulte, M.; Blake, D.; Hoehler, T.; McCollom, T. Serpentinization and its implications for life on the early Earth and Mars. *Astrobiology* **2006**, *6*, 364–376. [CrossRef] [PubMed]

19. Guillot, S.; Hattori, K. Serpentinites: Essential Roles in Geodynamics, Arc Volcanism, Sustainable Development, and the Origin of Life. *Elements* **2013**, *9*, 95–98. [CrossRef]

20. Okland, I.; Huang, S.; Dahle, H.; Thorseth, I.H.; Pedersen, R.B. Low temperature alteration of serpentinized ultramafic rock and implications for microbial life. *Chem. Geol.* **2012**, *318*, 75–87. [CrossRef]

21. Menez, B.; Pasini, V.; Brunelli, D. Life in the hydrated suboceanic mantle. *Nat. Geosci.* **2012**, *5*, 133–137. [CrossRef]

22. Sleep, N.H.; Bird, D.K.; Pope, E. Paleontology of Earth's Mantle. *Annu. Rev. Earth Planet. Sci.* **2012**, *40*, 277–300. [CrossRef]

23. Mayhew, L.E.; Ellison, E.T.; Miller, H.M.; Kelemen, P.B.; Templeton, A.S. Iron transformations during low temperature alteration of variably serpentinized rocks from the Samail ophiolite, Oman. *Geochim. Cosmochim. Acta* **2018**, *222*, 704–728. [CrossRef]

24. Templeton, A.S.; Ellison, E.T.; Glombitza, C.; Morono, Y.; Rempfert, K.R.; Hoehler, T.M.; Zeigler, S.D.; Kraus, E.A.; Spear, J.R.; Nothaft, D.B.; et al. Accessing the Subsurface Biosphere within Rocks Undergoing Active Low-Temperature Serpentinization in the Samail Ophiolite (Oman Drilling Project). *J. Geophys. Res.-Biogeosciences* **2021**, *126*, e2021JG006315. [CrossRef]

25. Alexander, E.B.; Coleman, R.G.; Keeler-Wolfe, T.; Harrison, S.P. *Serpentine Geoecology of Western North America: Geology, Soils, and Vegetation*; Illustrated Edition; Oxford University Press: Oxford, UK, 2006.

26. Olsen, A.A.; Bodkin, M.A.; Hausrath, E.M. Quantifying early mineral weathering reactions in serpentinite bedrock. *Appl. Geochem.* **2023**, *148*, 105543. [CrossRef]

27. Baumeister, J.L.; Hausrath, E.M.; Olsen, A.A.; Tschauner, O.; Adcock, C.T.; Metcalf, R.V. Biogeochemical weathering of serpentinites: An examination of incipient dissolution affecting serpentine soil formation. *Appl. Geochem.* **2015**, *54*, 74–84. [CrossRef]

28. Amrhein, C.; Suarez, D.L. The use of a surface complexation model to describe the kinetics of ligand-promoted dissolution of Anorthite. *Geochim. Cosmochim. Acta* **1988**, *52*, 2785–2793. [CrossRef]

29. Blum, A.E.; Stillings, L.L. Feldspar dissolution kinetics. In *Chemical Weathering Rates of Silicate Minerals*; White, A.F., Brantley, S.L., Eds.; Mineralogical Society of America: Washington, DC, USA, 1995; Volume 31, p. 583.

30. Cama, J.; Metz, V.; Ganor, J. The effect of pH and temperature on kaolinite dissolution rate under acidic conditions. *Geochim. Cosmochim. Acta* **2002**, *66*, 3913–3926. [CrossRef]

31. Manley, E.P.; Evans, L.J. Dissolution of feldspars by low-molecular-weight aliphatic and aromatic acids. *Soil Sci.* **1986**, *141*, 106–112. [CrossRef]

32. Mast, A.M.; Drever, J.I. The effect of oxalate on the dissolution rates of oligoclase and tremolite. *Geochim. Cosmochim. Acta* **1987**, *51*, 2559–2568. [CrossRef]

33. Stillings, L.L.; Drever, J.I.; Brantley, S.L.; Sun, Y.; Oxburgh, R. Rates of feldspar dissolution at pH 3–7 with 0–8 mM oxalic acid. *Chem. Geol.* **1996**, *132*, 79–89. [CrossRef]

34. Welch, S.A.; Ullman, W.J. The effect of organic acids on plagioclase dissolution rates and stoichiometry. *Geochim. Cosmochim. Acta* **1993**, *57*, 2725–2736. [CrossRef]

35. Olsen, A.A.; Rimstidt, D. Oxalate-promoted forsterite dissolution at low pH. *Geochim. Cosmochim. Acta* **2008**, *72*, 1758–1766. [CrossRef]

36. Hausrath, E.M.; Neaman, A.; Brantley, S.L. Elemental release rates from dissolving basalt and granite with and without organic ligands. *Am. J. Sci.* **2009**, *309*, 633–660. [CrossRef]

37. Brantley, S.L.; Olsen, A.A. Reaction Kinetics of Primary Rock-Forming Minerals under Ambient Conditions. In *Volume 7: Surface And Groundwater, Weathering and Soils*, 2nd ed.; Drever, J.I., Ed.; Elsevier: Amsterdam, The Netherlands, 2014.

38. Wolff-Boenisch, D.; Wenau, S.; Gislason, S.R.; Oelkers, E.H. Dissolution of basalts and peridotite in seawater, in the presence of ligands, and CO_2: Implications for mineral sequestration of carbon dioxide. *Geochim. Cosmochim. Acta* **2011**, *75*, 5510–5525. [CrossRef]

39. Bartlett, C.L.; Hausrath, E.M.; Adcock, C.T.; Huang, S.C.; Harrold, Z.R.; Udry, A. Effects of Organic Compounds on Dissolution of the Phosphate Minerals Chlorapatite, Whitlockite, Merrillite, and Fluorapatite: Implications for Interpreting Past Signatures of Organic Compounds in Rocks, Soils and Sediments. *Astrobiology* **2018**, *18*, 1543–1558. [CrossRef]

40. Hausrath, E.M.; Navarre-Sitchler, A.K.; Sak, P.B.; Williams, J.Z.; Brantley, S.L. Soil profiles as indicators of mineral weathering rates and organic interactions for a Pennsylvania diabase. *Chem. Geol.* **2011**, *290*, 89–100. [CrossRef]

41. Neaman, A.; Chorover, J.; Brantley, S.L. Element mobility patterns record organic ligands in soils on early Earth. *Geology* **2005**, *33*, 117–120. [CrossRef]

42. Neaman, A.; Chorover, J.O.N.; Brantley, S.L. Implications of the evolution of organic acid moieties for basalt weathering over geologic time. *Am. J. Sci.* **2005**, *305*, 147–185. [CrossRef]

43. Furrer, G.; Stumm, W. The role of surface coordination in the dissolution of delta-Al_2O_3 in dilute acids. *Chimia* **1983**, *37*, 338–341.

44. Sigg, L.; Stumm, W. The interaction of anions and weak acids with the hydrous goethite (alpha-feooh) surface. *Colloids Surf.* **1981**, *2*, 101–117. [CrossRef]

45. Kubicki, J.D.; Schroeter, L.M.; Itoh, M.J.; Nguyen, B.N.; Apitz, S.E. Attenuated total reflectance Fourier-transform infrared spectroscopy of carboxylic acids adsorbed onto mineral surfaces. *Geochim. Cosmochim. Acta* **1999**, *63*, 2709–2725. [CrossRef]

46. Oelkers, E.H.; Schott, J. Does organic acid adsorption affect alkali-feldspar dissolution rates? *Chem. Geol.* **1998**, *151*, 235–245. [CrossRef]

47. Martins, Z. Organic Chemistry of Carbonaceous Meteorites. *Elements* **2011**, *7*, 35–40. [CrossRef]

48. Botta, O.; Bada, J.L. Extraterrestrial organic compounds in meteorites. *Surv. Geophys.* **2002**, *23*, 411–467. [CrossRef]

49. Pizzarello, S.; Shock, E. The Organic Composition of Carbonaceous Meteorites: The Evolutionary Story Ahead of Biochemistry. *Cold Spring Harb. Perspect. Biol.* **2010**, *2*, a002105. [CrossRef]

50. Benner, S.A.; Devine, K.G.; Matveeva, L.N.; Powell, D.H. The missing organic molecules on Mars. *Proc. Natl. Acad. Sci. USA* **2000**, *97*, 2425–2430. [CrossRef]

51. Formisano, V.; Atreya, S.; Encrenaz, T.; Ignatiev, N.; Giuranna, M. Detection of methane in the atmosphere of Mars. *Science* **2004**, *306*, 1758–1761. [CrossRef]

52. Webster, C.R.; Mahaffy, P.R.; Atreya, S.K.; Flesch, G.J.; Mischna, M.A.; Meslin, P.-Y.; Farley, K.A.; Conrad, P.G.; Christensen, L.E.; Pavlov, A.A.; et al. Mars methane detection and variability at Gale crater. *Science* **2015**, *347*, 415–417. [CrossRef]

53. Webster, C.R.; Mahaffy, P.R.; Atreya, S.K.; Moores, J.E.; Flesch, G.J.; Malespin, C.; McKay, C.P.; Martinez, G.; Smith, C.L.; Martin-Torres, J.; et al. Background levels of methane in Mars' atmosphere show strong seasonal variations. *Science* **2018**, *360*, 1093–1096. [CrossRef]

54. Mumma, M.J.; Villanueva, G.L.; Novak, R.E.; Hewagama, T.; Bonev, B.P.; DiSanti, M.A.; Mandell, A.M.; Smith, M.D. Strong release of methane on Mars in northern summer 2003. *Science* **2009**, *323*, 1041–1045. [CrossRef]

55. Freissinet, C.; Glavin, D.P.; Mahaffy, P.R.; Miller, K.E.; Eigenbrode, J.L.; Summons, R.E.; Brunner, A.E.; Buch, A.; Szopa, C.; Archer, P.D.; et al. Organic molecules in the Sheepbed Mudstone, Gale Crater, Mars. *J. Geophys. Res.-Planets* **2015**, *120*, 495–514. [CrossRef] [PubMed]

56. Eigenbrode, J.L.; Summons, R.E.; Steele, A.; Freissinet, C.; Millan, M.; Navarro-Gonzalez, R.; Sutter, B.; McAdam, A.C.; Franz, H.B.; Glavin, D.P.; et al. Organic matter preserved in 3-billion-year-old mudstones at Gale crater, Mars. *Science* **2018**, *360*, 1096–1100. [CrossRef]

57. Millan, M.; Teinturier, S.; Malespin, C.A.; Bonnet, J.Y.; Buch, A.; Dworkin, J.P.; Eigenbrode, J.L.; Freissinet, C.; Glavin, D.P.; Navarro-Gonzalez, R.; et al. Organic molecules revealed in Mars's Bagnold Dunes by Curiosity's derivatization experiment. *Nat. Astron.* **2022**, *6*, 129–140. [CrossRef]

58. Scheller, E.L.; Hollis, J.R.; Cardarelli, E.L.; Steele, A.; Beegle, L.W.; Bhartia, R.; Conrad, P.; Uckert, K.; Sharma, S.; Ehlmann, B.L.; et al. Aqueous alteration processes in Jezero crater, Mars;implications for organic geochemistry. *Science* **2022**, *378*, 1105–1110. [CrossRef]

59. Sharma, S.; Roppel, R.; Murphy, A.; Beegle, L.W.; Bhartia, R.; Steele, A.; Razzell Hollis, J.; Siljestrom, S.; McCubbin, F.M.; Asher, S.A.; et al. Mapping Organic-Mineral Associations in the Jezero crater floor. In Proceedings of the American Geophysical Union Fall Meeting 2022, Chicago, IL, USA, 2–16 December 2022.

60. Steele, A.; Benning, L.G.; Wirth, R.; Schreiber, A.; Araki, T.; McCubbin, F.M.; Fries, M.D.; Nittler, L.R.; Wang, J.; Hallis, L.J.; et al. Organic synthesis associated with serpentinization and carbonation on early Mars. *Science* **2022**, *375*, 172–177. [CrossRef]

61. Steele, A.; Benning, L.G.; Wirth, R.; Siljestrom, S.; Fries, M.D.; Hauri, E.; Conrad, P.G.; Rogers, K.; Eigenbrode, J.; Schreiber, A.; et al. Organic synthesis on Mars by electrochemical reduction of CO_2. *Sci. Adv.* **2018**, *4*, eaat5118. [CrossRef]

62. Olsen, A.A.; Hausrath, E.M.; Rimstidt, J.D. Forsterite dissolution rates in Mg-sulfate-rich Mars-analog brines and implications of the aqueous history of Mars. *J. Geophys. Res.-Planets* **2015**, *120*, 388–400. [CrossRef]

63. King, P.L.; McLennan, S.M. Sulfur on Mars. *Elements* **2010**, *6*, 107–112. [CrossRef]

64. Carlson, R.W.; Johnson, R.E.; Anderson, M.S. Sulfuric acid on Europa and the radiolytic sulfur cycle. *Science* **1999**, *286*, 97–99. [CrossRef]

65. Bodkin, M.A. *Incipient Chemical Weathering of the Pine Hill Serpentinite, Little Deer Isle, ME*; Univeristy of Maine: Orono, ME, USA, 2013.

66. Zareian, M.; Ebrahimpour, A.; Bakar, F.A.; Mohamed, A.K.S.; Forghani, B.; Ab-Kadir, M.S.B.; Saari, N. A glutamic acid-producing lactic acid bacteria isolated from malaysian fermented foods. *Int. J. Mol. Sci.* **2012**, *13*, 5482–5497. [CrossRef] [PubMed]

67. Han, K.; Lim, H.C.; Hong, J. Acetic acid formation in escherichia coli formation. *Biotechnol. Bioeng.* **1992**, *39*, 663–671. [CrossRef] [PubMed]

68. Drake, H.L. *Acetogenesis, Acetogenic Bacteria, and the Acetyl-CoA "Wood/Ljungdahl" Pathway: Past and Current Perspectives*; Springer: Berlin/Heidelberg, Germany, 1994; pp. 3–60.
69. Lang, S.Q.; Butterfield, D.A.; Schulte, M.; Kelley, D.S.; Lilley, M.D. Elevated concentrations of formate, acetate and dissolved organic carbon found at the Lost City hydrothermal field. *Geochim. Cosmochim. Acta* **2010**, *74*, 941–952. [CrossRef]
70. R Core Team, T. *R: A Language and Environment for Statistical Computing*; R Foundation for Statistical Computing: Vienna, Austria, 2021.
71. Bowles, J.F.W.; Howie, R.A.; Vaughan, D.; Zussman, J. *Non-Silicates: Oxides, Hydroxides and Sulphides. (Rock-Forming Minerals.; No. 5A)*; Geological Society: Bath, UK, 2011.
72. Casey, W.H.; Westrich, H.R. Control of dissolution rates of orthosilicate minerals by divalent metal oxygen bonds. *Nature* **1992**, *355*, 157–159. [CrossRef]
73. Goyne, K.W.; Brantley, S.L.; Chorover, J. Effects of organic acids and dissolved oxygen on apatite and chalcopyrite dissolution: Implications for using elements as organomarkers and oxymarkers. *Chem. Geol.* **2006**, *234*, 28–45. [CrossRef]
74. Burgess, D.R. NIST SRD 46. Critically Selected Stability Constants of Metal Complexes: Version 8.0 for Windows, National Institute of Standards and Technology. 2004. Available online: https://data.commerce.gov/nist-srd-46-critically-selected-stability-constants-metal-complexes-version-80-windows (accessed on 25 February 2024).